Mem. S.A.It. Vol. 90, 216

Memorie della

The extragalactic population of neutron stars: the ULX paradigm revolution

G. L. Israel and G. A. Rodriguez Castillo, on beahlf of the UNSEEN collaboration

Istituto Nazionale di Astrofisica – Osservatorio Astronomico di Roma, Via Frascati 33, I-00078 Monte Posrzio Catone, Italy, e-mail: gianluca.israel@inaf.it

Abstract. The recent discovery of Ultraluminous X-ray Sources (ULXs) showing fast and rapidly evolving pulsations (PULXs) unambiguously associated these sources to accreting neutron stars (NSs) exceeding up to about 500 times their Eddington luminosity. These sources challenge our understanding of accretion physics and pose a key question about the nature of the ULXs as a class. The possible presence for a high magnetic field component close to the pulsar surface and the possible reason(s) for which a relatively small number of PULXs have been discovered so far is discussed. Furthermore, preliminary results from a search for new PULXs in the UNSEEN XMM-Newton project are shown.

Key words. accretion, accretion disks – galaxies: general – pulsars: general – stars: neutron – X-rays: binaries

1. Introduction

Ultraluminous X-ray sources are off-nuclear objects detected in nearby galaxies with X-ray luminosities in excess of 10^{39} erg s^{-1}, which is the Eddington luminosity ($L_{\rm Edd}$) for a black hole (BH) of 10 $M_{\odot}$ (Kaaret, Feng & Roberts 2017). $L_{\rm Edd}$ sets the upper limit to the accretion luminosity ($L_{\rm acc}$) that a compact object can steadily produce, since for $L_{\rm acc} > L_{\rm Edd}$, the accretion flow is halted by radiation pressure. For spherical accretion of fully ionized hydrogen, the limit for a NS can be written as $L_{\rm Edd} = 4\pi c G M m_{\rm p}/\sigma_{\rm T} \simeq 1.3 \times 10^{38}(M/M_{\odot})$ erg s^{-1}, where $\sigma_{\rm T}$ is the Thomson scattering cross section, $m_{\rm p}$ is the proton mass, and $M/M_{\odot}$ is the compact object mass in solar masses. Since early discoveries in the '70s with the Einstein mission (Fabbiano et al. 1992), the high luminosity of ULXs has been interpreted as accretion at or above the Eddington luminosity onto BHs of stellar origin (<80–100 $M_{\odot}$), or onto intermediate-mass (10^3–10^5 $M_{\odot}$) BHs (Poutanen et al. 2007; Zampieri et al. 2009).

The recent discovery of fast coherent pulsations with periods between 0.4 s and 32 s in the X-ray light curves of four distinct ULXs with luminosities in the $10^{39} \div 10^{41}$ erg s^{-1} range, unambiguously associate these ULXs with accreting NSs, therefore a compact object with mass of only $\sim$1.4$M_{\odot}$ or slightly larger (Bachetti et al. 2014; Füerst et al. 2016; Israel et al. 2017a,b; Carpano et al. 2018). These X-ray pulsars demonstrate that accreting NSs can attain extreme luminosities, above 500 times $L_{\rm Edd}$, which is hard to interpret in the context of standard accretion models successfully applied to other X-ray binaries. A significantly super-Eddington luminosity can be achieved if the magnetic field of the NS is in excess of about 10^{13}Gauss due to the reduction of the scatter-

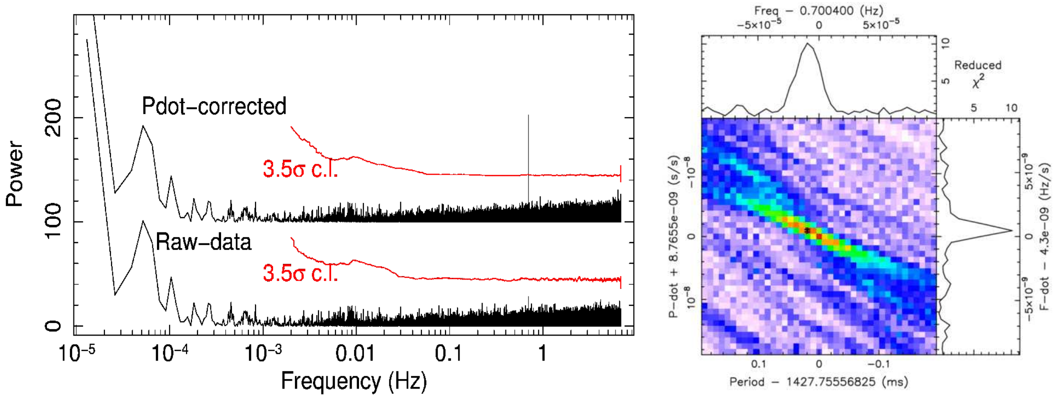

Fig. 1. Detection and study of the pulsations observed in the extreme pulsar NGC 5907 ULX. Left – Arbitrarily shifted (along the y-axis) power spectral density (PSD) of the 0.2-12 keV (XMM-Newton) NGC 5907 ULX light curves of the XMM-Newton archival observations carried out on 2003 February 20 before (lower PSD) and after (upper PSD) correcting the photon arrival times for the effect of a strong $\dot{P}$ component ($\sim 9\times10^{-9}$ s s^{-1}). Red curves mark the 3.5σ detection threshold for each PSD. Right – P versus $\dot{P}$ diagram used to refine the timing parameters of the pulsars. The figure clearly shows the importance of the correction: a small variation of ~5% with respect to the inferred $\dot{P}$ value is able to wash out the spin signal.

ing cross sections: a luminosity of $\sim 500\,L_{\rm Edd}$ would require a field strength of $> 10^{15}$ G (Mushtukov et al. 2015; Dall'Osso, Perna, & Stella 2015). However, the ~1 s rotation of the NS and its magnetosphere would drag matter at the magnetospheric boundary so fast that the centrifugal force would exceed the gravitational force, inhibiting the accretion on the NS surface by the so-called propeller mechanism (Illarionov & Sunyaev 1975; Stella, White & Rosner 1986). This problem can be mitigated by assuming that the emission is geometrically beamed (note that some degree of beaming must be present in all pulsars given that pulsations are observed) in the most extreme PULX, though an unrealistic beaming factor of 1/100 would be needed in the most extreme case of NGC 5907 ULX. Several new possible scenarios have been proposed in order to account for the PULX properties. The presence of a strong multipolar magnetic field ($\sim 10^{14}$ G) close to the surface of the NSs with a modest beaming appears a reasonable way out of the problem (Israel et al. 2017a; Chashkina, Abolmasov & Poutanen 2017); regardless to the latter component a dipolar component of the magnetic field is always present around the NS (of the order of 10^{11}-10^{13} Gauss) and channels the accretion stream toward its polar caps. The multipolar magnetic component is likely present in all NSs but it is difficult to be directly observed (for an example see Tiengo et al. 2013). However "standard" dipolar magnetic fields of $\sim 10^{12}$ G (with no additional multipolar components) are envisaged in other models (King, Lasota & Kluźniak 2017; King & Lasota 2019).

Another important consequence of the discovery of PULXs is that the nature of many ULXs, which have been classified in good faith as accreting black holes due to their high luminosity, is now in doubt. An unknown but possibly large fraction of ULXs might host an accreting NS rather than a BH, lso in consideration of the fact that not all the X-ray pulsar beams are pointing towards us, and therefore detectable. In general, the unambiguous identification of the nature of a NS in X-rays is achieved with the detection of rapid coherent signals reflecting the spin period of the NS. However, given the pulsed fractions (in the following we adopt the definition of semi-amplitude of the sinusoid divided by the source average count rate) observed in the PULXs this approach needs large count-statistics. The latter is currently available only for about ~15

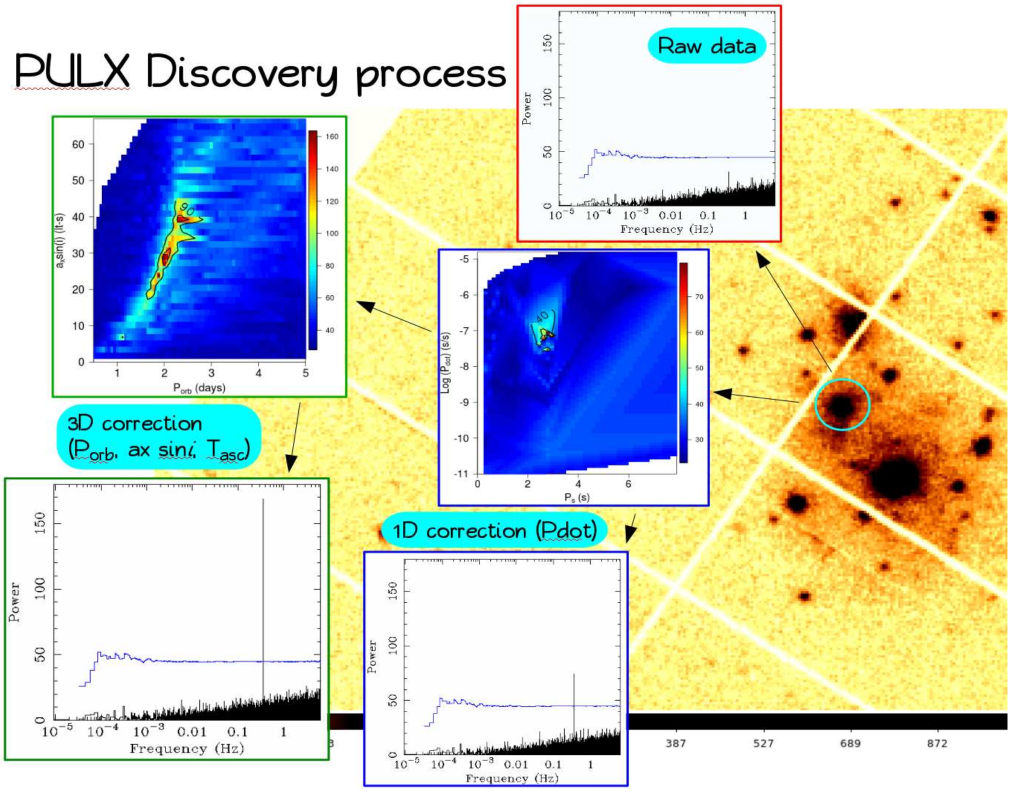

Fig. 2. Scheme of the signal discovery procedure adopted during the UNSEEN project. After the event extraction from a targeted ULX, an "uncorrected" PSD is carried out (red squared inset). Subsequently, a plot is obtained where each point in the plane corresponds to the power of the highest peak found in different PSD obtained by correcting the photon arrival times for a first period derivative component with values in the $-11 < \mathrm{Log}\dot{P} < -5$ range (blue squared insets). Colors mark the Leahy power estimates in the corresponding PSD (see intensity scale on the right). For the $\dot{P}$ value corresponding to the highest power estimate, a PSD is also shown. During the final step of the procedure the source photon arrival times are corrected for a Doppler effect originated by an orbital motion. We show the orbital period as a function of $a_{\rm X} \sin i$ together with the PSD corresponding to the orbital parameters providing the highest power of the PSD (green squared insets).

ULXs (among which are the four PULXs) out of the sample of about 300 known (Earnshaw et al. 2019); and remarkably, among all the ULXs with good enough statistics data sets, ~25% of them are proven to be NSs. On the other hand only one or two ULXs, out of 300, are reliable genuine black hole candidates due to the compact object dynamical mass measurement in the case of M101 X-1 (Liu et al. 2013), and due to low/hard high/soft spectral transitions and transient radio emission associate with them in the case of ESO 243-39 HLX-1 (Webb et al. 2013). Three known PULXs have PFs in the 10-15% range. However, counts collected in multiple, far apart observations, do not increase the signal search sensitivity, because of the orbital motion and the moderate-to-large $\dot{P}$ these sources have ($\dot{P} \sim 10^{-8} \div 10^{-11}$ s s^{-1}), which eventually washes out the signal too much to be corrected with reasonable searches.

Figure 1 clearly summarizes this issue: without a proper correction the signal of NGC 5907 ULX cannot be detected. To cope with this problem it is important to systematically and automatically sample a multi dimensional grid of timing parameters (up to six: the spin period P, its first derivative $\dot{P}$, the orbital period $P_{\rm orb}$, the semi major axis projection $a_{\rm X} \sin i$, and the time of the ascendent node $T_{\rm node}$). Due to the number of free parameters and grid step, up to 10^3–10^6 PSDs or periodograms are needed to complete the search analysis for a light curve. In order to speed up this otherwise time-consuming approach, it is possible to rely upon High Performance/Throughput Computers (HPCs/HTCs) which ensure a sensitive signal search over a large sample of light curves, maximizing the parameter resolution and with a relatively short execution time.

2. The UNSEEN project

It is evident, from the above considerations, that a major step forward in the study and understanding of ULXs goes through the expansion of the sample of ULXs where a sensitive search for pulsations can be carried out. With this aim we set up an observational program, carried out with XMM-Newton during AO17, aimed at doubling up the sample of ULXs with a good statistics where to identify and to study the ULX Neutron Star Extreme Extragalactic populatioN (UNSEEN). We started from the latest updated catalog of ULXs and super-Eddington off-nuclear X-ray sources detected by XMM-Newton in nearby galaxies (Earnshaw et al. 2019) and filtered objects according to the following criterion: **i)** to collect at least 10,000 photons within one XMM orbit (~135 ks), and **ii)** maximum visibility time per orbit larger than the requested time to collect the above counts. The final sample includes about 16 sources in 8 pointings for a total of about 30 sources with super-Eddington luminosities within the EPICs fields of view (FOVs). Condition **i)** was necessary in order to maximize the Nyquist frequency ($0.5\Delta t^{-1}$ where Δt is the time series sampling time, usually about 0.073 s for EPIC pn) for the signal search while keeping the maximum Fourier resolution (T^{-1}, where T is the observational timespan): the optimal approach for the search of coherent signals. Based on the current knowledge of the PULXs properties we expected to detect 1-3 new member of the class.

Figure 2 summarizes the systematic and automatic signal search procedure we adopted within the UNSEEN project. For each targeted ULX, coherent signals are first searched in raw data (with no corrections for the $\dot{P}$ or the orbital motion; red squared plot labelled "Raw data") by means of a Power Spectrum Density (PSD) where Fourier resolution and Nyquist frequency are maximized and the possible presence of non-Poissonian noise components is taken into account. If no signal is found during the first step, a grid of 1-dimension $\dot{P}$ values is applied to the source event times; for each $\dot{P}$ value a PSD is obtained and a corresponding plane P versus $\dot{P}$ is obtained as a function of the power estimates (see blue squared plots in Fig. 2 labelled "1D correction"; the shown PSD corresponds to the $\dot{P}$ value providing the highest power estimate). In the case reported in Figure 2 a significant peak is found above the 3.5σ detection threshold (blue solid line). Either or not a signal is found during this step a final analysis is carried out by assuming a 3-dimension grid of (circular) orbital parameters, i.e. the orbital period P_{orb}, the semi major axis projection $a_{\rm X} \sin i$, and the time of the ascendant node $T_{\rm node}$. Each tern of orbital parameters is used to modify the arrival times of source events and a PSD is carried out. In this case we are able to plot two parameters as a function of the PSD power estimate such that a first indication of P_{orb} and $a_{\rm X} \sin i$ is inferred (green squared plots labelled "3D correction").

2.1. M51 ULX7

M51 ULX7 was first detected with ROSAT observations at a luminosity above 10^{39} erg s^{-1}. The source is located at an offset of about 2.3 arcmin from the central AGN, close to the position of a young open cluster on a spiral arm of M51. Chandra observations showed flux variability ($\Delta L_{\rm X}/L_{\rm X} \geq 10$) and a ~7,620 s period modulation. A modulation was also observed in an XMM pointing at a significantly different period of ~5,900 s (Dewangan et al. 2005). The period variation argued against an orbital origin and suggested the presence of quasi periodic oscillations (QPOs). The XMM spectral properties and the fact that the source position is near a young massive star cluster with age $T \sim 12$ Myr (Abolmasov et al. 2007) suggested instead that M51 ULX7 is a high mass X-ray binary (HMXB). Based on a multi-wavelength approach (from radio to hard X-rays), it was proposed that the source might be an IMBH though an accreting NS could not be excluded (Earnshaw et al. 2016).

During three XMM pointings carried out between May and June 2018 we discovered coherent pulsations at a period of 2.8 s in the X-ray emission of M51 ULX7 (see Fig. 2). The pulse shape is sinusoidal and large variations of its amplitude were observed even within single exposures (pulsed fraction from less than 5% to 20%). The signal disappeared (3σ upper limits on the pulsed fraction of about 3%) for at least 3hr at the end of a XMM pointing. According to our analysis, the X-ray pulsar revolves in a 2-d orbital period binary with a projected semi-major axis $a_X \sin i \simeq 28$ lt-s (Rodriguez et al. 2019). For a neutron star of $1.4\,M_\odot$, this implies a lower limit on the companion mass of $8\,M_\odot$, placing the new system in the high-mass X-ray binary class. The pulsar is spinning-up at a rate $\dot{P} \simeq -1.5 \times 10^{-10} ss^{-1}$. Furthermore, in an archival 2005 XMM exposure, we measured a spin period of ~3.3 s, indicating a secular spin-up of $\dot{P}_{\rm sec} \simeq -10^{-9} ss^{-1}$, a value in the range of those detected in the other PULXs. Our findings suggest that the system consists of an OB giant and a moderately magnetic (dipole field component in the range 10^{12} G $\lesssim B_{\rm dip} \lesssim 10^{13}$ G) accreting NS with weakly beamed emission ($1/12 \lesssim b \lesssim 1/4$). Our analysis do not allow us to put any constraint on the possible presence of a multipolar component of the magnetic field close to the NS surface.

3. Conclusions

Though the search for new PULXs in the UNSEEN data is still on going, we note that with one new discovered member of the class we are consistent with our pre-analysis expectations. Nonetheless, the extreme variations on short time scales of the pulsed fraction of the 2.8 s signal of M51 ULX7 and the non detection of pulsations in several XMM datasets of M82 X-2 and NGC 5907 ULX, suggest that PULX signals might be even more difficult to detect than thought before and that more pointings of the same galaxies hosting ULXs are needed in order to have a higher chance of finding new pulsars. Correspondingly, also the number of NSs hosted by ULXs might be larger than estimated before.

References

Abolmasov, P. et al. 2007, Astr. Bull., 62, 36
Bachetti, M. et al. 2014, Nature, 514, 202
Carpano, S. et al. 2018, MNRAS, 476, L45
Chashkina A., Abolmasov, P. & Poutanen, J. 2017, ApJ, 308, 669
Dall'Osso, S., Perna, R. & Stella, L. 2015, MNRAS, 449, 2539
Dewangan, G.C. et al. 2005, ApJ, 635, 198
2016, MNRAS, 456, 3840
Earnshaw, H.P. et al. 2019, MNRAS, 483, 5554
Fabbiano, G. et al. 1992, ApJS, 80, 531
Füerst, F. et al. 2016, ApJ, 831, L14
Illarionov, A.F. & Sunyaev, R.A. 1975, A&A, 39, 185
Israel, G.L. et al. 2017a, Science, 355, 817
Israel et al. 2017b, MNRAS, 466, L48
Kaaret, Feng & Roberts, T. 2017, ARA&A, 55, 303
King, A., Lasota, J.-P., Kluźniak, W. 2017, MNRAS, 468, L59
King, A. & Lasota, J.-P. 2019, MNRAS, 485, 3588
Liu, J.F. et al. 2013, Nature, 503, 500
Mushtukov, A. et al. 2015 MNRAS, 454, 2539
Poutanen, Y. et al. 2007, MNRAS, 377, 1187
Rodriguez, G. et al. 2019, in preparation
Stella, L., White, N. E. & Rosner, R. et al. 1986, ApJ, 308, 669
Tiengo, A. et al. 2013, Nature, 500, 312
Webb, N. et al. 2013, Science, 337, 554
Zampieri, L. et al. 2009, MNRAS, 400, 677